The Astrophysical Journal, 979:52 (5pp), 2025 January 20 https://doi.org/10.3847/1538-4357/ada123

Advancing CO_2^{++} Modeling in the Martian Dayside Ionosphere: Insights from Natural Lifetime Analysis

Long Cheng[1], Erik Vigren[1], Moa Persson[1], Hao Gu[2], and Jun Cui[2]
[1] Swedish Institute of Space Physics, Uppsala, Sweden; long.cheng@irf.se
[2] School of Atmospheric Sciences, Sun Yat-Sen University, Zhuhai, People's Republic of China
Received 2024 November 04; revised 2024 December 07; accepted 2024 December 14; published 2025 January 17

Abstract

The molecular dication CO_2^{++} has, as previously reported, been detected in the Martian ionosphere by the Neutral Gas and Ion Mass Spectrometer on the Mars Atmosphere and Volatile Evolution (MAVEN) mission. Photochemical models have also been developed to reproduce the CO_2^{++} density in the Martian dayside ionosphere but underestimate significantly the observations. In this study, we examine the influence of the CO_2^{++} natural lifetime against spontaneous dissociation on its modeled density. We show that extending the assumed CO_2^{++} lifetime significantly reduces the discrepancy between the photochemical model predictions and MAVEN observations. Specifically, when treating CO_2^{++} as stable against natural dissociation, instead of invoking a lifetime of 4 s as done in previous studies, the data-to-model ratio comes close to unity throughout the altitude range 160–220 km. We argue that stability of CO_2^{++} against natural dissociation does not necessarily conflict with results from a frequently cited experimental investigation. Our study provides new insights for advancing photochemical modeling of the Martian ionosphere and underscores the need for further laboratory measurements targeting fundamental properties of doubly charged ions.

Unified Astronomy Thesaurus concepts: Planetary ionospheres (2185); Mars (1007); Space plasmas (1544); Ionization (2068)

1. Introduction

Doubly charged ions have been studied in various planetary ionospheres, including those of Earth, Venus, Mars, and Titan (R. Thissen et al. 2011). O. Witasse et al. (2002, 2003) predicted the presence of a CO_2^{++} layer in the Martian atmosphere, assuming photochemical equilibrium. C. Simon et al. (2005) predicted and modeled N_2^{++}, O_2^{++}, and O^{++} in Earth's ionosphere, validating their O^{++} modeling by comparisons with measurements from the satellite Atmosphere Explorer. J. Lilensten et al. (2005) predicted a N_2^{++} layer in Titan's upper atmosphere. G. Gronoff et al. (2007) modeled O^{++}, CO_2^{++}, and N_2^{++} in the Venusian ionosphere, finding good agreement between their modeled O^{++} densities and Pioneer Venus Orbiter measurements (H. A. Taylor et al. 1980). However, detecting minor doubly charged ions in planetary ionospheres remains challenging. Until recently, only atomic O^{++} ions had been measured in the ionospheres of Earth (E. L. Breig et al. 1977, 1982), Venus (J. L. Fox & G. A. Victor 1981), and Io (L. A. Frank et al. 1996) and S^{++} ions in the ionosphere of Io (L. A. Frank et al. 1996).

H. Gu et al. (2020) reported on the first detection of CO_2^{++} in the Martian ionosphere from measurements by the Neutral Gas and Ion Mass Spectrometer (NGIMS; P. R. Mahaffy et al. 2015) on the Mars Atmosphere and Volatile Evolution (MAVEN; B. M. Jakosky et al. 2015) mission. This marked the first detection of molecular dications in any planetary ionosphere. Using a multi-instrumental MAVEN data set, H. Gu et al. (2020) also carried out photochemical modeling to predict the CO_2^{++} density in the Martian dayside ionosphere. However, the model underestimated the density by a factor of >2 at low altitudes (~160 km) and by a factor of >30 at high altitudes (~220 km). Even when accounting for the photoionization (PI) of CO_2^{+}, the results remain underestimated by an order of magnitude at higher altitudes. Similarly, earlier modeling results from O. Witasse et al. (2003) also show a degree of underestimation when compared with the recent MAVEN observations. These discrepancies point toward inaccuracies in the current modeling of CO_2^{++} in the Martian ionosphere.

Previous studies used the assumption of a 4 s natural lifetime of CO_2^{++} against spontaneous dissociation, based on the laboratory measurements conducted nearly 30 yr ago in a storage ring experiment (D. Mathur et al. 1995). However, it is noted that the authors argued that the ultimate destruction of the ions was due to interactions with residual gases in the ring. As such, the assumption of a 4 s natural lifetime is questionable. In this study, we aim to explore how variations in the assumed natural lifetime of CO_2^{++} influence the modeled CO_2^{++} densities in the Martian dayside ionosphere. Reevaluating the impact of this parameter on current models may provide important insights into the validity of utilized assumptions. The work of H. Gu et al. (2020) is at the heart of our methodology as explained in Section 2. Results are presented and discussed in Section 3, and a summary with concluding remarks is provided in Section 4.

2. Method

According to O. Witasse et al. (2002, 2003) and G. Gronoff et al. (2007), the production of CO_2^{++} includes (1) double PI of CO_2 and (2) double electron-impact-ionization (EI) of CO_2. The destruction of CO_2^{++} occurs through (1) dissociative recombination (DR) with free electrons, (2) reactions with CO_2, (3) reactions with O, and (4) natural dissociation. The CO_2^{++}

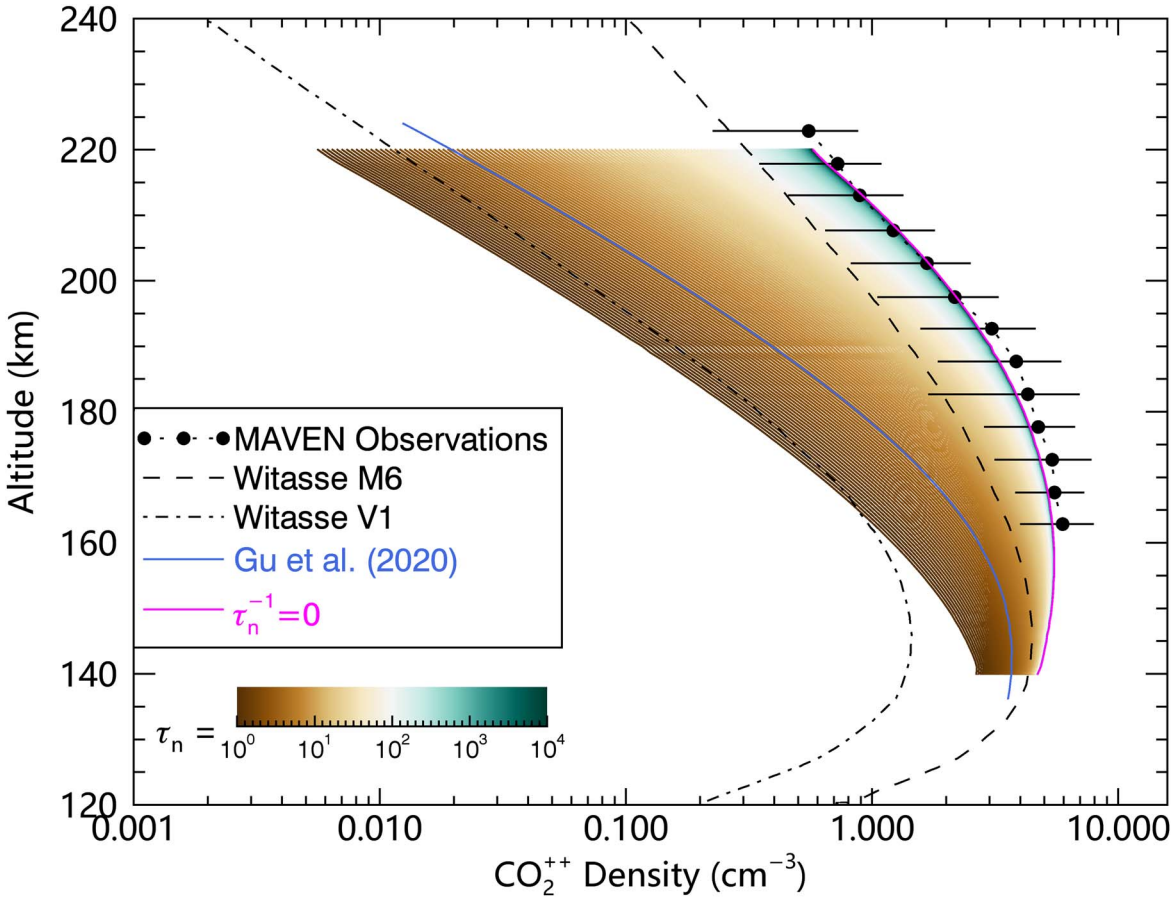

Figure 1. CO_2^{++} density profiles in the Martian upper dayside atmosphere from MAVEN observations with standard deviations (points with error bars), extracted from the work of H. Gu et al. (2020). Also shown are modeling results from O. Witasse et al. (2003) for the Mariner 6 (M6) conditions (dashed line) and Viking 1 (V1) conditions (dashed–dotted line), as well as the results from the MAVEN-based model of H. Gu et al. (2020; blue line), wherein $\tau_n = 4$ s was assumed. How model results of H. Gu et al. (2020) would be if considering different fixed values of τ_n is illustrated by lines with colors corresponding to the color bar, ranging from 1 to 10^4 s. The magenta line indicates the model result with $\tau_n^{-1} = 0$, which neglects the natural dissociation of CO_2^{++}.

density in photochemical equilibrium is derived from

$$n_{CO_2^{2+}} = \frac{P_{CO_2}^{PI} + P_{CO_2}^{EI}}{\tau_n^{-1} + n_e k_{dr} + n_{CO_2} k_{CO_2} + n_O k_O}, \quad (1)$$

where $P_{CO_2}^{PI}$ and $P_{CO_2}^{EI}$ are the production rates via double PI and EI of CO_2; n_e, n_{CO_2}, and n_O are the number densities of electrons, CO_2, and O; k_{dr} is the DR rate coefficient; k_{CO_2} and k_O are the rate coefficients for reactions of CO_2^{++} with CO_2 and O, respectively; and τ_n is the CO_2^{++} natural lifetime against spontaneous dissociation.

Our work leans on the work of H. Gu et al. (2020), and we refer readers to their Section 3 for a detailed description of their retrieval of the individual terms appearing in Equation (1). In short, the average CO_2, O, and electron density profiles in that work were calculated from NGIMS and Langmuir Probe and Waves (L. Andersson et al. 2015) data, and rate coefficients for k_{dr}, k_{CO_2}, and k_O were set based on the works of K. Seiersen et al. (2003), O. Witasse et al. (2002), and G. Gronoff et al. (2007), respectively. For k_{dr} and k_{CO_2}, dependencies on the electron and neutral temperature were considered, respectively. The term τ_n^{-1} was simply set to 0.25 Hz with reference to the work of D. Mathur et al. (1995), and the production rate of CO_2^{++} due to double PI and double EI of CO_2 were derived from CO_2 densities, with relevant (measurement-based) photon and suprathermal electron fluxes and cross-section data compiled by T. Masuoka (1994) and Y. Itikawa (2002).

The blue line in Figure 1 shows the resulting modeled CO_2^{++} density of H. Gu et al. (2020) when they limited CO_2^{++} production to double PI and EI of CO_2. The profile was extracted from Figure 1 of H. Gu et al. (2020). Seeking to explain the data–model discrepancy, H. Gu et al. (2020) added to their default model CO_2^{++} production through PI of CO_2^+. We believe that the approach applied by H. Gu et al. (2020) to calculate that contribution is inaccurate and suspect that it gives too high values. Our reasoning is as follows: The unattenuated PI frequency of CO_2 at 1 au varies with solar activity, approximately ranging from 8 to 22×10^{-7} Hz (W. F. Huebner & J. Mukherjee 2015). At Mars, this corresponding ionization frequency falls in the range $\sim$3–12×10^{-7} Hz, also depending on the heliocentric distance. The ionization energy of CO_2 is 13.78 eV (e.g., L. S. Wang et al. 1988), while the energy required to remove an additional electron from CO_2^+ is $\sim$22 eV, inferred from a threshold of $\sim$36 eV for the double ionization process of CO_2 (e.g., J. A. R. Samson et al. 1977). The significantly higher energy requirement for removing a second electron suggests that the solar EUV-driven electron removal frequency from CO_2^+ should be markedly lower than the PI frequency of neutral CO_2. This is the case for multiple other species where ionization frequencies for both neutral and ionized versions have been derived (W. F. Huebner &

J. Mukherjee 2015). Figure 2(a) of H. Gu et al. (2020) shows an average CO_2^+ concentration of $\sim 10^3\ cm^{-3}$ at an altitude of 200 km. It follows that the production rate of CO_2^{++} from the PI of CO_2^+ in this region should be limited to $\sim 10^{-3}\ cm^{-3}\ s^{-1}$ and possibly be significantly lower. Based on this, we argue that the PI of CO_2^+ plays a much less significant role in producing CO_2^{++} than suggested by Figure 2(c) of H. Gu et al. (2020). Hence, we only consider the production of CO_2^{++} via double PI and EI of CO_2 in this work.

If underestimated production does not contribute notably to the fact that the modeled CO_2^{++} densities are lower than the densities observed, it can be suspected that something instead is off with the CO_2^{++} loss terms in the model. In Figure 2(d) of H. Gu et al. (2020), it can be seen that the natural dissociation of CO_2^{++} is the leading loss term for altitudes exceeding 150 km. From the altitude profiles of $P_{CO_2}^{PI}$, $P_{CO_2}^{EI}$ (Figure 2(c) of H. Gu et al. 2020), and $n_{CO_2^{++}}$ (black solid line in Figure 1 of H. Gu et al. 2020) generated with the assumption of $\tau_n = 4$ s), it is straightforward to assess via Equation (1) how the modeled CO_2^{++} density changes with the assumed value of τ_n.

3. Results

We generated various CO_2^{++} density profiles by adjusting τ_n from 1 to 10^5 s. The results are shown in Figure 1, where the color bar represents the line color corresponding to different τ_n values. We also included the result from MAVEN observations (H. Gu et al. 2020) with standard deviations within altitude bins (points with error bars), modeling results from O. Witasse et al. (2003) for the Mariner 6 (M6) conditions (dashed line) and Viking 1 (V1) conditions (dashed–dotted line), as well as from H. Gu et al. (2020) based on MAVEN data (blue line). Overall, previous modeling efforts consistently underestimated the CO_2^{++} density. Using a τ_n of 4 s, H. Gu et al. (2020) underestimated CO_2^{++} densities by a factor of 2 at 160 km and by a factor of 35 at 220 km. When we set τ_n to 1 s, the modeled CO_2^{++} densities decrease, deviating more from MAVEN observations as CO_2^{++} ions are removed more rapidly. As we increased τ_n from 1 to 10^2 s, the modeled CO_2^{++} densities increase significantly, aligning more closely with MAVEN data. While we further increase τ_n from 10^2 to 10^4 s, the model CO_2^{++} slightly increases. Under the extreme assumption of an infinite natural lifetime, which effectively removes the τ_n term in Equation (1) (as $\tau_n^{-1} = 0$), the modeled results align very well with MAVEN observations (see the magenta line).

In Figure 1, it can be seen that the model results of O. Witasse et al. (2003) for M6 conditions are not that far from the NGIMS observations. However, this agreement is partially coincidental. The modeling by O. Witasse et al. (2003) relied on neutral densities and temperatures from the Mars Thermosphere General Circulation Model (S. W. Bougher et al. 1999, 2000), as well as electron densities, temperatures, and double ionization rates from the 1D Mars ionospheric model of O. Witasse (2000), which could yield a wide range of predicted densities. During the M6 flyby, Mars was near perihelion, at a heliocentric distance of 1.43 au (within its range of 1.38–1.67 au), and experiencing high solar activity, with an F10.7 index of 166 (~65 during low solar activity and ~200 during high solar activity). These conditions contributed to the higher predicted CO_2^{++} densities under M6 geophysical settings. Hence, we emphasize that the model results based on NGIMS neutral data and relevant illumination conditions are more meaningful for direct comparison with the NGIMS ion data set.

Figure 2 presents a map showing the ratio between the CO_2^{++} densities from MAVEN observations and those predicted by the photochemical model across various τ_n values, at various altitudes. The color scale represents the magnitude of the ratio, with darker colors indicating larger discrepancies. A ratio closer to 1 signifies a better model prediction of the observations. For a given τ_n, the discrepancy tends to increase with altitude, while for a given altitude, the discrepancy decreases as τ_n increases. Profiles where the model-to-data ratio equals 10, 5, and 2 are marked by yellow, red, and magenta lines, respectively. To reduce the model underestimation to a factor of 5 at an altitude of ~220 km, a τ_n value between 20 and 30 s is required, while a τ_n value of around 100 s is necessary to bring the underestimation down to a factor of 2.

Table 1 presents the data–model ratios for various τ_n values across altitudes ranging from ~160 to ~220 km. For a τ_n value of 4 s, the ratio is ~2 at the lower altitude and increases to ~30 at the upper altitude. The ratios decrease by about half for a τ_n value of 10 s. When τ_n is increased to 50 and 100 s, the model results become more comparable to MAVEN observations below 200 km, with ratios of only 3 and 2 at around 200 km, respectively. Under the assumption of an infinite lifetime ($\tau_n^{-1} = 0$), the model results are closely aligned with MAVEN observations across all altitudes, as also illustrated in Figure 1.

4. Summary and Discussion

In this study, we modeled CO_2^{++} densities in the Martian dayside ionosphere by considering photochemical equilibrium, accounting for production via double PI and double EI of CO_2 and destruction through natural dissociation, DR, and reactions with CO_2 and O. We utilized altitude profiles of plasma quantities from H. Gu et al. (2020), based on MAVEN observations. We argued that the PI of CO_2^+ should be negligible. We proposed an analysis of CO_2^{++} natural lifetime to investigate its impacts on modeled CO_2^{++} densities. Our findings show that the discrepancy between photochemical model predictions and MAVEN observations decreases as the CO_2^{++} lifetime is assumed to be longer. Compared to the modeling results with $\tau_n = 4$ s, increased τ_n to 20, 50, and 100 s reduces the data–model ratio from 2 to 1 at ~160 km altitudes and from ~30 to 6, 3, and 2 at ~220 km altitudes. While extending τ_n further continues to reduce the data–model discrepancy, the effect becomes less pronounced.

Our findings suggest that the natural lifetime of CO_2^{++} may be significantly longer than the ~4 s assumed in previous modeling efforts (e.g., O. Witasse et al. 2003; G. Gronoff et al. 2007; H. Gu et al. 2020). While the assumption of a lifetime of ~4 s was based on results reported from a storage ring experiment (D. Mathur et al. 1995), it is noted that the authors of that study stress that the destruction of the stored ions was driven not only by natural dissociation but also, and possibly predominantly, by collisions with residual gases. Hence, we are not questioning the experimental work of D. Mathur et al. (1995) itself but rather the interpretation of their results in subsequent studies. In reality, the experiment only demonstrated that the ions had a measured lifetime of ~4 s in the storage ring, where they experienced high-energy collisions with residual gases. This ~4 s value represents merely a lower limit of the natural lifetime, leaving the possibility that the true lifetime against unimolecular decay could be several tens of

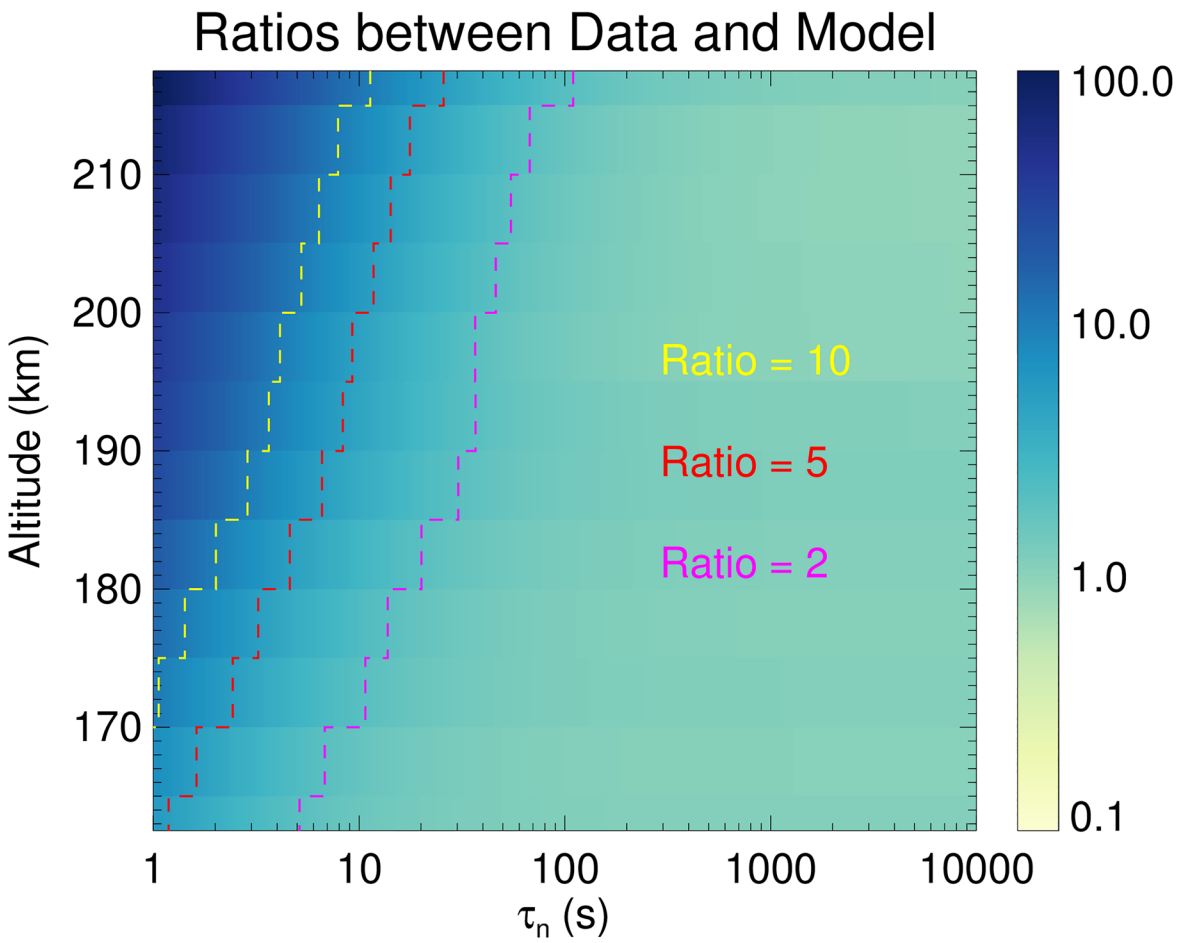

Figure 2. A map showing the ratios between CO_2^{++} densities from MAVEN observations (H. Gu et al. 2020) and those predicted by the photochemical model of H. Gu et al. (2020), calculated for various values of CO_2^{++} natural lifetime (τ_n) at different altitudes. The ratios are represented by the accompanying color bar. The yellow, red, and magenta lines indicate values of τ_n at various altitudes where the data–model ratios equal to 10, 5, and 2, respectively.

Table 1
Ratios of CO_2^{++} Density from MAVEN Observations (H. Gu et al. 2020) to Modeling Results with Varying τ_n Values, at Various Altitudes

	$\tau_n = 4$ s	$\tau_n = 10$ s	$\tau_n = 20$ s	$\tau_n = 50$ s	$\tau_n = 100$ s	$\tau_n = \infty$
$h = 217.5$ km	26.44	11.18	6.14	3.09	2.09	1.08
$h = 212.5$ km	18.95	8.11	4.53	2.37	1.66	0.94
$h = 202.5$ km	12.86	5.71	3.35	1.92	1.45	0.98
$h = 192.5$ km	9.25	4.36	2.74	1.77	1.44	1.12
$h = 182.5$ km	5.61	2.90	2.01	1.47	1.29	1.11
$h = 172.5$ km	3.49	2.06	1.59	1.31	1.21	1.12
$h = 162.5$ km	2.26	1.56	1.33	1.19	1.14	1.10

seconds or even longer. It would be rewarding with new investigations targeting the natural lifetime of CO_2^{++} ions, ideally at a facility, such as the Double Electrostatic Ion Ring Experiment (H. T. Schmidt et al. 2013), offering improved vacuum conditions (compared with the experiment of D. Mathur et al. 1995) and/or the possibility to easily vary the background pressure.

Naturally, there are, in addition to τ_n several other parameters, the assigned values which affect the modeled CO_2^{++} density in the Martian ionosphere. H. Gu et al. (2020) estimated that, accounting for uncertainties in rate coefficients, ionization cross sections, solar irradiance, and neutral and ion densities, the predicted CO_2^{++} density may deviate from the observed density by no more than three standard deviations. However, these uncertainties cannot account for the significant discrepancies observed at higher altitudes. A comprehensive review of all input relevant for the CO_2^{++} balance in the Martian dayside ionosphere is also beyond the scope of the present work. The specific targeting of the natural lifetime against unimolecular decay was motivated upon realization that results from the experimental work of D. Mathur et al. (1995) have, as addressed above, not necessarily been correctly interpreted in subsequent modeling studies.

Also, the model used in this work does not take into consideration transport processes, warranting further investigations of the CO_2^{++} balance through models that incorporate both photochemistry and transport dynamics (e.g., M. Mayyasi et al. 2019; J. L. Fox et al. 2021). Nevertheless, our findings indicate that the natural lifetime of CO_2^{++} may require reevaluation, as longer lifetimes could significantly improve

the accuracy of current photochemical models in replicating observed CO_2^{++} densities in the Martian ionosphere.

Acknowledgments

We are grateful for the support from the Swedish National Space Agency (Dnr 2022–00201). The MAVEN NGIMS data are publicly available at the MAVEN Archive Page (https://atmos.nmsu.edu/data_and_services/atmospheres_data/MAVEN/ngims.html).

ORCID iDs

Long Cheng https://orcid.org/0000-0003-0578-6244
Erik Vigren https://orcid.org/0000-0003-2647-8259
Moa Persson https://orcid.org/0000-0003-3497-3209
Hao Gu https://orcid.org/0000-0002-9831-0618
Jun Cui https://orcid.org/0000-0002-4721-8184

References

Andersson, L., Ergun, R. E., Delory, G. T., et al. 2015, SSRv, 195, 173
Bougher, S. W., Engel, S., Roble, R. G., & Foster, B. 1999, JGR, 104, 16591
Bougher, S. W., Engel, S., Roble, R. G., & Foster, B. 2000, JGR, 105, 17669
Breig, E. L., Torr, M. R., & Kayser, D. C. 1982, JGRA, 87, 7653
Breig, E. L., Torr, M. R., Torr, D. G., et al. 1977, JGR, 82, 1008
Fox, J. L., Benna, M., McFadden, J. P., & Jakosky, B. M. 2021, Icar, 358, 114186
Fox, J. L., & Victor, G. A. 1981, JGR, 86, 2438
Frank, L. A., Paterson, W. R., Ackerson, K. L., et al. 1996, Sci, 274, 394
Gronoff, G., Lilensten, J., Simon, C., et al. 2007, A&A, 465, 641
Gu, H., Cui, J., Niu, D. D., et al. 2020, E&PP, 4, 396
Huebner, W. F., & Mukherjee, J. 2015, P&SS, 106, 11
Itikawa, Y. 2002, JPCRD, 31, 749
Jakosky, B. M., Lin, R. P., Grebowsky, J. M., et al. 2015, SSRv, 195, 3
Lilensten, J., Witasse, O., Simon, C., et al. 2005, GeoRL, 32, L03203
Mahaffy, P. R., Benna, M., King, T., et al. 2015, SSRv, 195, 49
Masuoka, T. 1994, PhRvA, 3886, 50
Mathur, D., Andersen, L. H., Hvelplund, P., Kella, D., & Safvan, C. P. 1995, JPhB, 28, 3415
Mayyasi, M., Narvaez, C., Benna, M., Elrod, M., & Mahaffy, P. 2019, JGRA, 124, 3786
Samson, J. A. R., Kemeny, P. C., & Haddad, G. N. 1977, CPL, 51, 75
Schmidt, H. T., Thomas, R. D., Gatchell, M., et al. 2013, RScI, 84, 055115
Seiersen, K., Al-Khalili, A., Heber, O., et al. 2003, PhRvA, 68, 022708
Simon, C., Lilensten, J., Dutuit, O., et al. 2005, AnGeo, 23, 781
Taylor, H. A., Brinton, H. C., Bauer, S. J., et al. 1980, JGRA, 85, 7765
Thissen, R., Witasse, O., Dutuit, O., et al. 2011, PCCP, 13, 18264
Wang, L. S., Reutt, J. E., Lee, Y. T., & Shirley, D. A. 1988, JESRP, 47, 167
Witasse, O. 2000, PhD thesis, Univ. Joseph–Fourier–Grenoble I
Witasse, O., Dutuit, O., Lilensten, J., et al. 2002, GeoRL, 29, 104
Witasse, O., Dutuit, O., Lilensten, J., et al. 2003, GeoRL, 30, 1360